

GROSEN K.H., KOUSTED, M., TREICHEL, S.L

21. JUNE - 2021

MASTER'S

THESIS



AALBORG UNIVERSITET
SPECIALE IDRÆTSTEKNOLOG

2-dimensional tennis serves shows similar successful mechanical parameter across physiological differences

GROSEN K.H., KOUSTED, M., TREICHEL, S.L.

*Sports Technology 4th-Semester, Department of Health Science and Technology, Aalborg University, Aalborg, Denmark
Email: 21gr10203@hst.aau.dk*

Purpose: A 2-Dimensional collision and flight model was developed, to investigate the stroke parameters on successful serves regarding different physiological capabilities.

Method: The investigation was carried out using a 2-Dimensional forward dynamics simulation by computing a collision and flight model.

Results: Main findings were the optimum impact angles regarding spin rate of 36° , 35° and 34° for professional, recreational and junior. The optimum impact angle could be achieved at multiple racket face angles across all three players. Additionally, impact angles larger than optimum resulted in an accelerated velocity decrease.

Conclusions: Almost similar impact angles, considering the physiological differences between the players, will make it simple for players and coaches to implement high spin rates for topspin serves.

Keywords: Tennis serve, Computer simulation, Forward dynamic

1. INTRODUCTION

The evolution of sports equipment has propelled the game of tennis forward. The change from wooden rackets to rackets made from composite material enabled engineers to 1) reduce the weight 2) increase the racket head size and 3) increase the frame stiffness. All factors that makes it possible for elite players to commonly produce serves at 200 kph [2]. Millions of tennis players around the world are trying to master the technique of the “perfect” serve. The international Tennis Federation (ITF) reported in 2017 about 87 million tennis players globally. This evolution over the last 30 years has led to an increased amount of research on the game of tennis [15]. Howard Brody was one of the first to look into the physics in the game of tennis in the 80’s [1]. He showed how delicate tennis can be, especially during a tennis serve. When neglecting external forces acting on the ball in flight, the racket face angle at collision can only vary about two degrees and the interval gets even smaller with lower impact heights or greater racket velocities [1]. To increase the range of possible racket face angles the player can choose to use a spin serve by applying an impact angle [5]. The magnitude of the racket velocity combined with the impact and racket face angle are the main mechanical factors that will determine the outcome of a tennis serve [5]. There are countless

ways the mechanical factors can be combined to achieve a successful serve. Though, for competitive tennis players the key is to make the returner unable to return the serve with high ball velocity and spin rate [3]. This eliminates some of the combinations of mechanical factors, but still leaves many combinations to be analyzed.

To analyse these combinations and find the limitations of the tennis serve, forward dynamics can be used [9]. This is seen as good method to grasp the complexity of tennis [21]. Computer simulations are an approximation of the real world, hence assumptions are made to limit the computational capacity of the simulation. The tricky part is to obtain the complexity-sweet-spot so the conclusions can be applied to the real world [24].

For the forward dynamics simulation of a tennis serve, two primary models must be developed - a collision and a flight model [13], [15], [22].

The collision model is important to incorporate the physics of impact between the racket and the tennis ball, and will constrain the possible outcomes of the ball trajectory [22].

Collisions between tennis balls and rackets have been studied extensively by authors both experimental and theoretical [4], [8], [9], [11], [12]. Using different methods, they all tried to quantify different aspects of

the collision such as damper coefficients, spring stiffness, contact time, coefficient of restitution and coefficient of friction to evaluate the rebound properties of the ball. For example, Ghaednia et al. [8] recorded the collision using a high speed camera capable of capturing 10,000 frames per second, and Goodwill et al. [12] used the finite element method for collision simulations.

For the study of ball trajectories, Metha et al. [18] covered several studies which investigated the aerodynamic properties of tennis balls using wind tunnel experiments.

Using computational models will make it possible to evaluate a large number of tennis serve outcomes by investigating small variations of an isolated mechanical factor while keeping the rest of the mechanical factors constant. By understanding these individual factors it is possible to aid players and coaches understand factors to accomplish a successful serve in the game of tennis.

Specifically, this paper is investigating the impact and racket face angle to obtain a successful serve for different physiological capabilities regarding professional, recreational and junior tennis players.

2. METHODS

The 2D collision and flight model for investigating tennis serve outcomes was programmed in Python. The model consisted of a simple time-integration contrary to more powerful numerical solutions, such as the Runge-Kutta time-integration, which is possible with small time steps ($dt = 1 * 10^{-4}s$) [11]. The orientation of the collision model is based on the coordinate system of the racket, while the coordinate system of the flight model was based on the global coordinate system (figure 4).

2.1. Aerodynamics

For a realistic simulation of the ball trajectory, aerodynamics is important. Three different forces influence the ball while in flight: 1) gravitational acceleration (mg) 2) drag force (F_D) and 3) Magnus force (F_M). While mg remains constant throughout the flight, F_D depends on the ball velocity with F_M also being dependent on the angular velocity of the ball in flight. For calculating the magnitude of F_D and F_M the following equations were used:

$$F_D = \frac{1}{2}C_D A \rho v^2 \quad (1)$$

and

$$F_M = \frac{1}{2}C_L A \rho v^2 \quad (2)$$

Where ρ is the density of the air, A is the cross-sectional area of the tennis ball, v is the initial ball velocity while C_D and C_L are coefficients of drag and lift, respectively. Both coefficients are dimensionless. For $v < 33.8$ (m/s) C_D will change slightly, for instance when hitting a ground stroke from the baseline in tennis, but for tennis serves an acceptable approximation is

that C_D is constant because of high ($v > 33.8$ m/s) ball velocities [19]. C_L on the other hand will increase with increasing angular velocity [18] and the magnitude of C_L was found using the following equation:

$$C_L = \frac{1}{2 + \frac{v}{r\omega}} \quad (3)$$

Where ω is the angular velocity and r is the radius of the tennis ball. Cross [5] reported that a positive C_L results in backspin and a negative C_L results in topspin. Furthermore, C_D will increase with increasing spin rate. The magnitude of the increase of C_D was quantified using Stepanek [23]:

$$C_D = 0.55 + \frac{1}{[22.5 + 4.2(\frac{v}{r\omega})^h]^p} \quad (4)$$

Where h and p are constant values of 2.5 and 0.4, respectively.

2.2. Collision

To constrain the outcomes of the ball trajectory a collision model was developed. Perpendicular (x -values) and tangential (y -values) forces were computed using matrices. To simplify the analytical process, the model assumed that the impact always was at the geometrical center of the string bed. The model contained a racket assumed to be rigid, thus neglecting vibration losses of the racket at impact, and a tennis ball. For the perpendicular values, a spring and damper were added to the ball in parallel with a spring being added to the string bed in series with the spring of the ball [11] (figure 1).

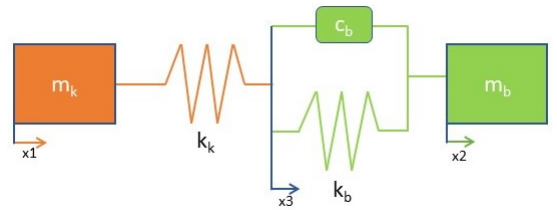


FIGURE 1: *Perpendicular spring and damper model of the present study. m_k is the mass of the racket, x_1 is the position of the racket, k_k is the spring constant of the string bed, c_b is the damping coefficient of the tennis ball, k_b is the spring of the tennis ball, x_3 is the position of the intersection between k_k and k_b , m_b is the mass of the tennis ball and x_2 is the position of the tennis ball.*

The damper accounts for the energy loss that occurs because of hysteresis of the tennis ball. From experimental procedures, the damping effect of the string bed is negligible [17]. The spring stiffness (k_k) of the string bed will not only vary depending on the string type, string tension and head size [11], but

also depending on the applied force. Authors have found the stiffness of the string bed to be between 30 kN/m and 100 kN/m ranging from 200 N and 1200 N applied force, respectively [16], [17]. Optimally, k_k for a specific string bed would be found experimentally, given the above, but the present study did not have access to appropriate apparatus, hence values from previous studies were used. Here, Goodwill and Haake [11] found a lower limit of 40 kN/m and upper limit of 60 kN/m by applying a distributed force perpendicular to the string plane. These constant values were in good agreement with experimental values. To quantify the perpendicular magnitude of the tennis ball spring stiffness (k_b) and damper coefficient (c_b), equations from Goodwill and Haake [11] were used:

$$k_b = \frac{m_b \pi^2}{T_c^2} \quad (5)$$

and

$$c_b = -\frac{2m_b}{T_c} \ln(COR) \quad (6)$$

Where m_b is the mass of the tennis ball, T_c is contact time and COR is coefficient of restitution. Both c_b and k_b are dependent on the impact velocity due to the fact that T_c and COR is included in equations 5 and 6. Experimental data of T_c and COR from Haake et al. [14] were used to estimate c_b and k_b .

k_k , k_b and c_b will only be active as long as contact between the racket and tennis ball is maintained (figure 1). To acquire the spring and damper force while also knowing the distribution of deformation between the racket and the tennis ball, the following three differential equations were used on the basis of figure 1:

$$m_k \ddot{x}_1 = -(x_1 - x_3)k_k \quad (7)$$

$$m_b \ddot{x}_2 = (x_3 - x_2)k_b + (\dot{x}_3 - \dot{x}_2)c_b \quad (8)$$

$$m_k \ddot{x}_1 = -m_b \ddot{x}_2 \quad (9)$$

Where \ddot{x}_1 and \ddot{x}_2 are the acceleration of the racket and ball, respectively, while \dot{x}_2 and \dot{x}_3 are the velocity of the ball and intersection between k_k and k_b , respectively. Equation 9 accounts for the distribution of deformation by applying equilibrium of the system in figure 1.

To eliminate double integration from the model, and in doing so reducing the differential system from a second order to a first order system, two new differential equations were derived:

$$x_4 = \dot{x}_1 \Rightarrow \dot{x}_4 = \ddot{x}_1 \quad (10)$$

$$x_5 = \dot{x}_2 \Rightarrow \dot{x}_5 = \ddot{x}_2 \quad (11)$$

Substituting these into equations 7-9 yields five coupled first order differential equations:

$$\begin{bmatrix} \dot{x}_1 \\ \dot{x}_2 \\ \dot{x}_3 \\ \dot{x}_4 \\ \dot{x}_5 \end{bmatrix} = \begin{bmatrix} 0 & 0 & 0 & 1 & 0 \\ 0 & 0 & 0 & 0 & 1 \\ \frac{k_k}{c} & \frac{k_b}{c} & -\frac{(k_k+k_b)}{c} & 0 & 1 \\ -\frac{k_k}{m_k} & 0 & \frac{k_k}{m_k} & 0 & 0 \\ \frac{k_k}{m_b} & 0 & -\frac{k_k}{m_b} & 0 & 0 \end{bmatrix} \begin{bmatrix} x_1 \\ x_2 \\ x_3 \\ x_4 \\ x_5 \end{bmatrix} \quad (12)$$

From these coupled differential equations, the time integration procedure of the program can be stated. Expanding the collision model to 2 dimensions, similar equations can be formulated for the tangential values, representing the effect of the the tangential force F_f of the collision.

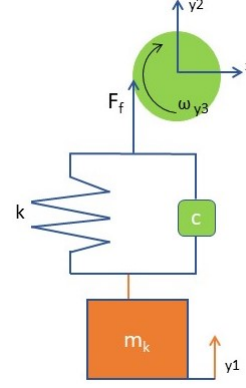


FIGURE 2: Tangential spring and damper model of the present study. y_1 is the position of the racket, k is the combined spring of the racket and ball, c is the damping coefficient of the tennis ball, F_f is the tangential force, y_2 is the position of the tennis ball and y_3 is angular position of the tennis ball.

Contrary to the perpendicular model, the tangential model had a combined spring stiffness for racket and ball (k) in parallel with a damper (c) (figure 2). Goodwill et al. [12] reported that both k and c are lower for oblique impacts compared to normal impacts. First, the ball stiffness is decreased because of a lower and longer lasting reaction force during impact [12] and second, the string bed stiffness is assumed lower tangentially than perpendicularly - hence k was 50% less than k_b . The decrease of c is due to the fact that COR is 4% higher for oblique impacts [12]. Furthermore, angular dimensions (y_3 , \dot{y}_3 and \ddot{y}_3) were added. Three differential equations were used on the basis of figure 2 to quantify the forces of the system:

$$m_k \ddot{y}_1 = -(y_1 - y_2 - r y_3)k - (\dot{y}_1 - \dot{y}_2 - \dot{y}_3)c \quad (13)$$

$$m_b \ddot{y}_2 = -m_k \ddot{y}_1 \quad (14)$$

$$I \ddot{y}_3 = r m_b \ddot{y}_2 \quad (15)$$

Where $I = \frac{2}{3} m_b r^2$ is the moment of inertia of the ball, r is the radius of the ball and \ddot{y}_3 is the angular acceleration of the ball. This differential system was also reduced from a second order to first order system by substitution of three new equations:

$$y_4 = \dot{y}_1 \Rightarrow \dot{y}_4 = \ddot{y}_1 \quad (16)$$

$$y_5 = \dot{y}_2 \Rightarrow \dot{y}_5 = \ddot{y}_2 \quad (17)$$

$$y_6 = \dot{y}_3 \Rightarrow \dot{y}_6 = \ddot{y}_3 \quad (18)$$

Rearranging the six differential equations for \dot{y}_n results in the following system of differential equations:

$$\begin{bmatrix} \dot{y}_1 \\ \dot{y}_2 \\ \dot{y}_3 \\ \dot{y}_4 \\ \dot{y}_5 \\ \dot{y}_6 \end{bmatrix} = \begin{bmatrix} 0 & 0 & 0 & 1 & 0 & 0 \\ 0 & 0 & 0 & 0 & 1 & 0 \\ 0 & 0 & 0 & 0 & 0 & 1 \\ -\frac{k}{m_k} & \frac{k}{m_k} & \frac{kr}{m_k} & -\frac{c}{m_k} & \frac{c}{m_k} & \frac{cr}{m_k} \\ \frac{k}{m_b} & -\frac{k}{m_b} & -\frac{kr}{m_b} & \frac{c}{m_b} & -\frac{c}{m_b} & -\frac{cr}{m_b} \\ \frac{kr}{I} & -\frac{kr}{I} & -\frac{krr}{I} & \frac{cr}{I} & -\frac{cr}{I} & -\frac{crr}{I} \end{bmatrix} \begin{bmatrix} y_1 \\ y_2 \\ y_3 \\ y_4 \\ y_5 \\ y_6 \end{bmatrix} \quad (19)$$

With the perpendicular and tangential differential equations, the model could estimate the distribution of perpendicular (F_N) and tangential forces (F_f) when racket velocity, impact angle (α) and racket face angle (β) were given. An α of zero would result in only perpendicular forces being exerted to the ball. An α different from zero would exert both perpendicular and tangential forces to the ball, which would increase the tangential velocity and spin rate and decrease the perpendicular velocity of the ball. In figure 3 the distribution of forces can be seen.

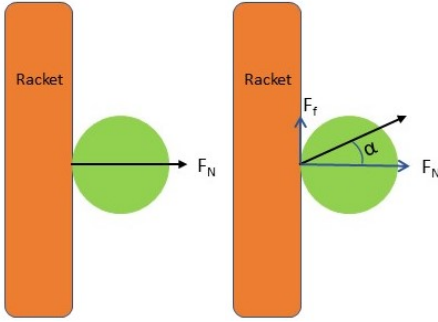


FIGURE 3: *Left: α of zero would result in only perpendicular forces (F_N) being exerted to the ball. Right: An α different from zero would exert both perpendicular (F_N) and tangential forces (F_f) to the ball. In both examples β is zero.*

At the end of the impact, the ball would either slide or roll of the string bed [10]. In tribology, this scenario is referred to as stick-slip.

To take stick-slip behaviour in the racket-ball contact into account, a limitation was computed for F_f , called F_{lim} :

$$F_{lim} = \dot{x}_4 m_b \mu, \quad (20)$$

Where \dot{x}_4 is the acceleration of the ball and $\mu = 0.35$ is the coefficient of friction between strings and ball. If F_f exceeds F_{lim} , F_f is then returned to F_{lim} , which means the ball slips/slides, while if it does not exceed, the ball will experience rolling.

As mentioned in the beginning of this section, two different coordinate systems were used for the collision and flight model as seen in figure 4. In order to transform the values from the local coordinate system

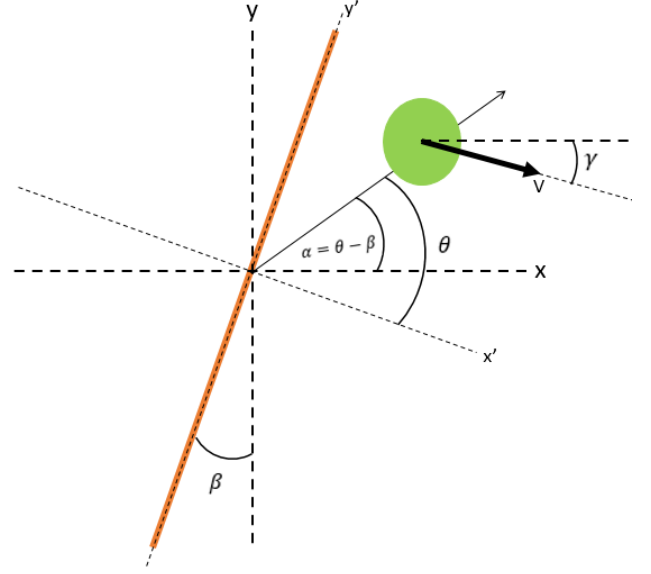


FIGURE 4: *Orientation of the local coordinate system for the racket (x' and y') and global coordinate system for the flight of the ball (x and y). α was found by subtracting the two simulation inputs θ and β . v is the initial ball velocity dependent on the racket velocity, α and β and has an angle γ relative to x .*

of the collision model to the global coordinate system of the flight model, the velocity components (v_x and v_y) were multiplied with a rotation matrix:

$$\begin{bmatrix} v'_x \\ v'_y \end{bmatrix} = \begin{bmatrix} \cos(\beta) & \sin(\beta) \\ -\sin(\beta) & \cos(\beta) \end{bmatrix} \begin{bmatrix} v_x \\ v_y \end{bmatrix} \quad (21)$$

2.3. Numerical Simulation Scenarios

To specify a successful serve and to narrow down the unlimited possibilities into a realistic simulation, three players with difference in physiological capabilities were established - Professional, recreational and junior. Individual constant values of impact heights were 3, 2.8 and 2.2 m, respectively, while racket velocities were 40, 30 and 25 m/s, respectively [2], [6]. Air density ρ (1.22 kg/m^3), perpendicular racket stiffness (50 kN/m), coefficient of friction μ (0.35), gravitational acceleration (9.82 m/s^2), ball radius (0.033 m), mass (0.059 kg) and mass of the racket (0.2 kg) were constant during all simulations.

In order to obtain all successful serves for each player, the collision model simulated all possible combinations of α and β with angle steps of 1 degree in the interval 0 through 90 degrees. The outputs from the collision model (v'_x , v'_y and ω) and the impact height were then implemented in the flight model to compute the ball trajectory. The radius of the ball was added to the height of the net (0.943 m) and the distance from impact point to service line (18.318 m). These dimensions corresponds to a serve down the middle of

Successful serves								
Professional	$\beta(^{\circ})$	$\alpha(^{\circ})$	RPM	v (m/s)	X (m)	Y (m)	$\gamma(^{\circ})$	n
Flat	8–10	0–7	0–1036	56.5–56.9	16.39–18.12	0.97–1.30	-8.2 – -6.1	10
Topspin	9–24	16–68	3237–6914	22.2–54.9	14.09–18.31	0.95–2.77	-6.6 – 10.3	223
Recreational								
Flat	6–9	0–8	0–1150	42.3–42.6	16.01–18.30	0.95–1.43	-6.7 – -3.4	15
Topspin	9–22	21–60	3237–5294	22.2–40.5	14.23–18.31	0.95–2.57	-3.9 – 10.3	199
Junior								
Flat	3–6	0–9	0–1151	35.2–35.5	16.00–18.24	0.95–1.36	-2.9 – 0.3	17
Topspin	7–17	23–53	3250–4470	22.7–33.6	14.28–18.31	0.96–2.39	0.6 – 12.3	150

TABLE 1: The values for a successful serve, where β is the racket face angle, α is the impact angle, RPM is topspin rotation velocity in revolutions per minute, v is the initial ball velocity on the basis of v'_x and v'_y , X the location of contact with the court, Y the ball clearance over the net, γ is the initial angle of v relative to horizontal with negative indicating below and positive above and n is the number of successful serves.

the court and was used to segregate the unsuccessful serves. Furthermore, to characterize flat and topspin serves cut-off values were established: flat < 1200 RPM and spin rate > 3200 RPM [20].

One optimum flat and one optimum topspin serve was selected from the successful flat and topspin serves for each player in order to show ball trajectory examples. The requirements were a high v while landing as close to service line as possible for the flat serve. Additionally, the topspin serve was required to have peak spin rate.

3. RESULTS

Table 1 indicates that the professionals have the most options for a successful topspin serve ($n = 223$) and juniors the least ($n = 150$). Additionally, the junior has the most options for a flat serve ($n = 17$), and professional the least ($n = 10$).

γ for the three players tends to vary greater for topspin serves than flat serves (table 1). While the junior has to perform with γ above the global x-axis (figure 4) for a topspin serve to be successful, the recreational and professional can perform with γ above and below. Additionally, for the flat serve all players requires to perform with γ in a negative direction, except for the junior, which has successful serves just above the horizontal direction 0.3.

Table 1 reveals that v is greater for flat serves compared to topspin serves. Furthermore, professional and recreational requires a v of at least 22.2 m/s and 22.7 m/s for junior players in order to produce a successful topspin serve.

Topspin serves have a greater Y compared to flat serves with the professional achieving the greatest $Y = 2.77$, while similar trends are seen for the values of X with topspin serves being able to land shorter in the service box than the flat serve (table 1).

Figures 5 and 6 add additional knowledge to the information given in table 1 regarding α and β . Figure 5 shows v and spin rate for flat and topspin serves at a

given α , which increases with increased racket velocity. Peak spin rate is found at an α of 34° , 35° and 36° for junior, recreational and professional, respectively. α post peak spin rate will entail a larger decrease in v compared to pre peak spin. Figure 6 shows the range of possible α for flat and top spin serves at a given β , which shifts right with increased impact height and racket velocity. The largest range of possible α for a topspin serve is found at a β of 14° , 18° and 21° for junior, recreational and professional, respectively. For a flat serve the largest range of possible α is found at a β of 4° , 8° and 9° for junior, recreational and professional, respectively. A gap between two α -intervals at a given β denotes the serve is too long. α -values below the minimum α , that corresponds to a successful serve, denotes the serve is too short. Likewise, α -values above the maximum α denotes either the cut-off value of 3200 RPM has been reached or that the serve is too short. The stars in figure 6 indicates the optimum flat and topspin serves represented in figures 7-9.

The ball trajectories for the optimum flat and topspin serves for each player are represented in figures 7, 8 and 9. The flat serves tends to have a lower net clearance than topspin serves. While the spin rate varies for each player the α remained at $35^{\circ} \pm 1$ for all players. β -values of 14° , 18° and 21° for junior, recreational and professional, respectively, are equal to the ones represented in figure 6 with largest range of possibly successful serves.

4. DISCUSSION

A 2-Dimensional collision and flight model was developed, to investigate the stroke parameters on successful serves regarding different physiological capabilities.

The simulated initial ball velocities of the present study for successful professional flat serves (56.5–56.9 m/s) were similar to the values from studies that described the dimensional ball kinematics by elite male tennis players, (Sakurai et al. [20], $52.0 \pm 2.9 m/s$; Chow

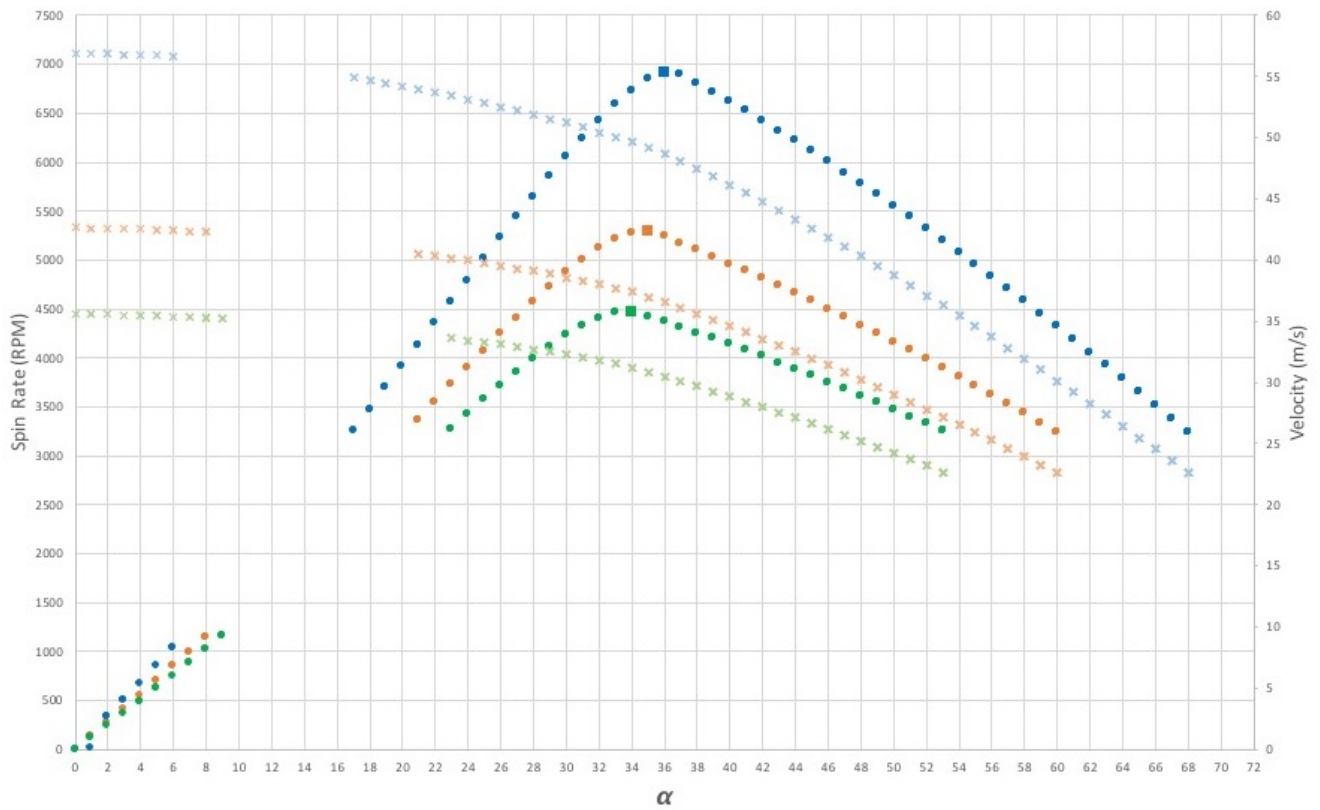


FIGURE 5: Ball velocity (cross) and spin rate (circle) as a function of α . Blue represents professional, orange is recreational and green is junior. The square indicates peak spin rate. $\alpha < 10$ are flat serves.

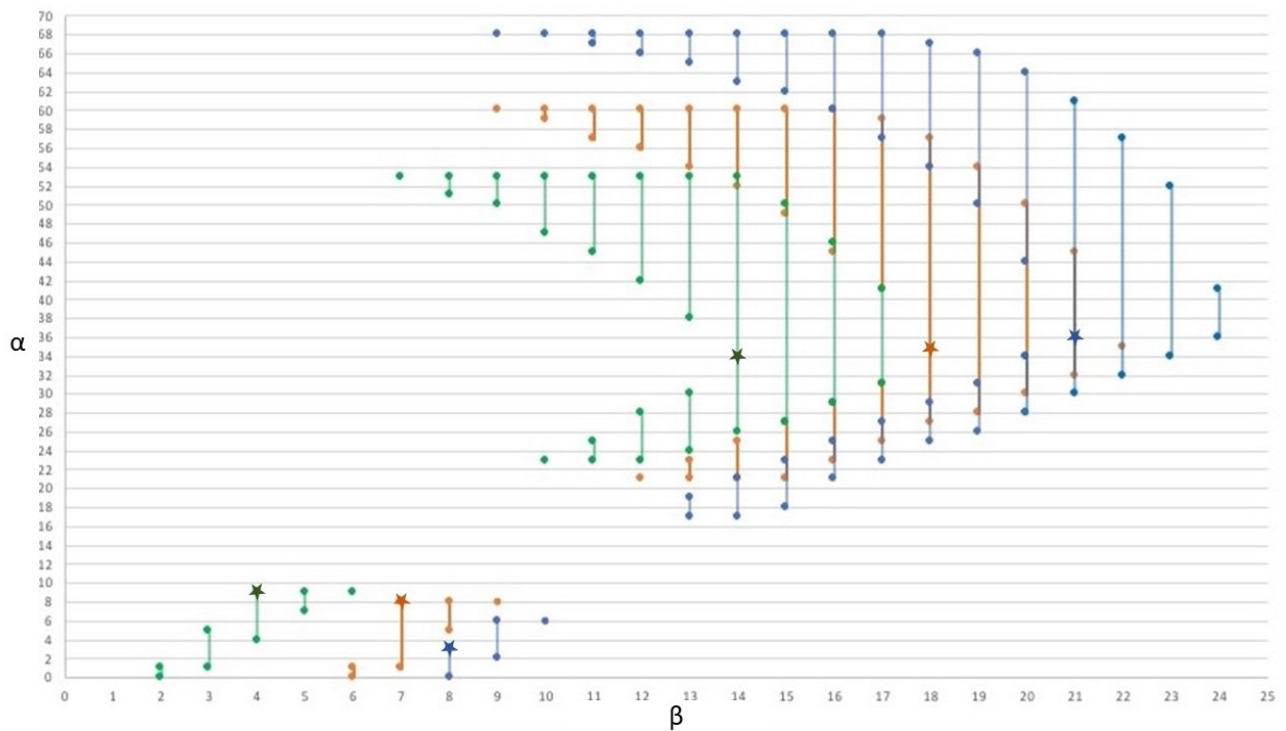


FIGURE 6: The range of possible α at a given β for successful serves. Blue represents professional, orange is recreational and green is junior. $\alpha < 10$ are flat serves.

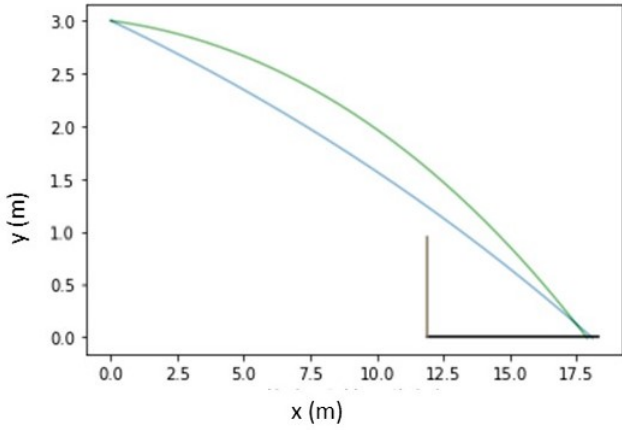


FIGURE 7: Optimum flat (blue) and topspin (green) tennis serves for professional. $\beta = 8^\circ$, $\alpha = 3^\circ$, $\gamma = -6.8^\circ$, spin rate = 501 RPM, $v = 56.8$ m/s, $Y = 1.25$ m and $X = 18.12$ m for the flat serve.
 $\beta = 21^\circ$, $\alpha = 36^\circ$, $\gamma = -1.9^\circ$, spin rate = 6914 RPM, $v = 48.7$ m/s, $Y = 1.61$ m and $X = 17.91$ m for the topspin serve.

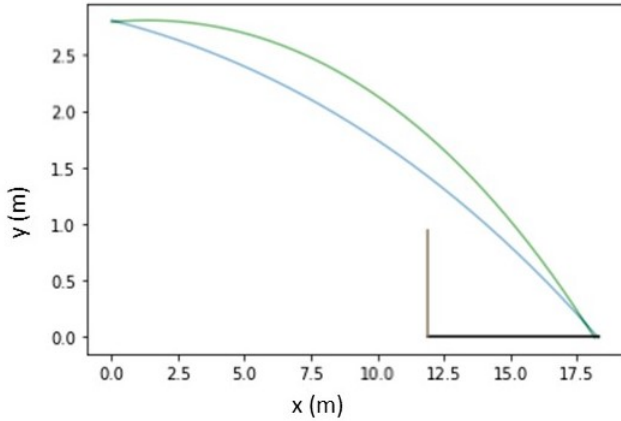


FIGURE 8: Optimum flat (blue) and topspin (green) tennis serves for recreational. $\beta = 7^\circ$, $\alpha = 8^\circ$, $\gamma = -3.4^\circ$ spin rate = 1150 RPM, $v = 42.3$ m/s, $Y = 1.42$ m and $X = 18.30$ m for the flat serve.
 $\beta = 18^\circ$, $\alpha = 35^\circ$, $\gamma = 1.3^\circ$ spin rate = 5294 RPM, $v = 36.98$ m/s, $Y = 1.80$ m and $X = 18.18$ m for the topspin serve.

et al. [3], 51.1 ± 3 m/s; Fleisig et al. [7], 50.8 ± 4 m/s). The initial racket velocity (40 m/s) represented in this study were similar with those represented by Chow et al. [3], (38.57 ± 2.33 m/s). This indicates that the simulation in this study developed serve velocities corresponding to those found by professional players in real match conditions. On the other hand, producing a serve without spin is only possible through simulations, as [20] reported a minimum spin rate of 678 RPM. One thing not incorporated in the present model is the ball release, as the vertical ball position is often higher than

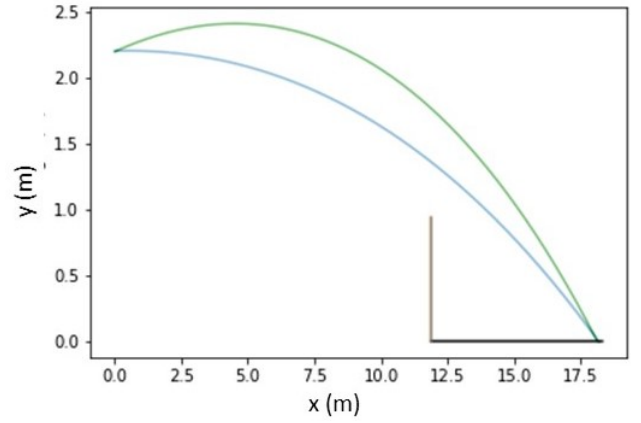


FIGURE 9: Optimum flat (blue) and topspin (green) tennis serves for junior. $\beta = 4^\circ$, $\alpha = 9^\circ$, $\gamma = 0.3^\circ$ spin rate = 1152 RPM, $v = 35.2$ m/s, $Y = 1.37$ m and $X = 18.24$ m for the flat serve.
 $\beta = 14^\circ$, $\alpha = 34^\circ$, $\gamma = 5.3^\circ$, spin rate = 4470 RPM, $v = 31.22$ m/s, $Y = 1.77$ m and $X = 18.14$ m for the topspin serve.

the inevitable impact point [2]. This will mean that the ball has a vertical velocity at impact, which will increase the spin rate [5].

The peak spin rate for topspin serves (6914 RPM) did not correspond well with those found in Pallis et al., 1998, (4651 RPM) nor those found in Sakurai et al. [20], (3705 RPM), where spin rates is overestimated in the present study for topspin serves. Since the values in the tangential axis are not corresponding well with existing literature, an assumption could be that the tangential stiffness and damper are at fault. While the perpendicular stiffness and damper can be found with simple drop-tests [11], tangential stiffness and damper requires extensive apparatus in order to grasp the oblique impact phenomenon between a tennis racket and ball [8]. On the other hand, maybe players from these studies (Chow et al. [3]; Sakurai et al. [20]; Fleisig et al. [7]; and Pallis et al., 1998) could favor from the results regarding α and β of the present study to increase the spin rate of their serve. Additionally, even though spin rates are overestimated in the present study, it is believed that the spin rate pattern, as a function of α from figure 5, is realistic.

As it appears in figures 7, 8 and 9, the flat serves have a more direct trajectory than those for the topspin serves. In addition, the results presented in table 1 show that the velocities for the flat serves are higher than for the topspin serves, as expected. Combined with a bounce close to the service line (18.318 m), the reaction time will be reduced for the opponent compared to a topspin serve, which is a good incentive to go for the flat serve. However, the limits in the present study means that there are no data on the behavior of the ball after it bounces off the tennis court, and the higher and less

predictable bounce from the spin serve is known to be challenging for the returner. Worth noting is that the margin of error is lower for performing a flat serve than performing a topspin serve. Looking at the values for β and α in table 1, the range of these, in relation to achieve a successful serve, is considerably smaller than for a topspin serve. This is elaborated by the number of successful serves for both professional, recreational and junior players, with $n = 10$, $n = 15$ and $n = 17$, respectively. Hence, it will be more likely that even small deviations may have bigger consequences at the attempt of a flat serve. On the other hand, the margin of error in the attempt of performing a topspin serve in comparison is higher based on the ranges of β , α and number of successful serves (table 1).

From table 1, successful topspin serves of $v = 22.2m/s$ can be seen. Despite the fact that such a serve is approved as a successful serve, this is far from an optimum serve as the low velocity of the ball, probably gives the opponent favorable conditions for returning the serve [5]. Luckily, in the game of tennis, the server has two attempts to initiate the point which favors players who can produce high racket velocities to 1) perform a flat serve with high ball velocities and if that fails 2) perform a topspin serve with a high spin rate and larger margin of error.

Chow et al. [3] reported the importance of high racket velocity for both flat and topspin serves. This statement can also be observed in figure 5 when distinguishing between the three players. If the professional player chose to use the same racket velocity as the junior player, both the maximum ball velocity and spin rate would decrease.

As Brody [1] found, our model predicted that β can only vary 1 degree for a completely flat serve ($\alpha = 0$), even though our model contained drag force and gravitational acceleration (figure 6). The fact that only one β -value results in a successful serve proves that β is dependent on impact height and velocity [1]. This highlights the necessity of the player's ability to accelerate the ball angularly to increase the range of possible β . In order to achieve this, the player must have an $\alpha > 0$. An increase of α will increase spin, as stated in figure 5, until a peak value is obtained which will then entail a decrease in spin with increasing α . The nature of this can be explained by F_N and F_f , if Coulomb friction is assumed, by applying:

$$F_f \leq F_N \mu. \quad (22)$$

For all players in figure 5 at $\alpha > 36^\circ$ the velocity decrease as a function of α accelerates due to the energy loss from sliding friction. As stated in equation 22, increasing μ will also entail larger F_f , as illustrated by the infamous spaghetti string technique, which is now banned by ITF [4].

The optimum α regarding spin rate is found at 34° , 35° and 36° for junior, recreational and professional, respectively (figure 5). It is interesting that even

with large physiological differences between the three players the optimum α regarding spin rate is $35^\circ \pm 1$. Additionally, the parabola-like feature of the spin rate in figure 5 entails that a 1 degree shift from the optimum α will still result in a high spin rate. Furthermore, these values can be achieved at multiple β -values across all three players, as seen in figure 6.

As stated in table 1, the junior can only achieve a successful topspin serve with a positive γ -value. This can help juniors to understand why they must serve slightly upwards to make the serve successful. If the serve outcome is too long, it would need more spin done by increasing α (figure 5).

Figure 6 is seen as a useful tool for tennis players and coaches for visual explanation and is advised to be combined with video footage during training sessions. This will enable players and coaches to understand and fine-adjust α and β to improve the serve and in turn improve match performance. For example, from slow-motion video footage it is observed that β is about 11° and α is about 36° for the junior player of the present study. Three different options are then present for the player to achieve a successful serve: 1) increase α , 2) decrease α or 3) increase β . First option will result in a low velocity topspin serve (figure 5), second option will result in a high velocity topspin serve (figure 5) with a small margin of error and the third option will eventually entail the player to have a large range of successful α if a β of 14° is reached. Furthermore, figure 6 will also explain that greater impact height and racket velocity will result in a bigger gap between the lowest successful α and the highest. This will make it possible for the professional players of the present study to vary their serve to a greater extent compared to the recreational and junior player.

For future work, the 2-D collision and flight model can be expanded to 3-D, which will mean the width of the tennis court will also come into play. Adding to the possibilities of the ball trajectory, it will also add to the players positioning options behind the baseline. Furthermore, it will be possible to simulate spin axes with 3-D directions to analyse the slice serve and the interplay between topspin and sidespin. One thing to consider is that the successful flat and topspin serves found in the present 2-D study, would have a small margin of error since serves in 3-D would be unsuccessful if hit wide of the service box.

To accommodate the discussion of the margin of error to the net and service line a player should aim for, it may be beneficial to perform a Monte Carlo simulation. By simulating a large number of serves, a Monte Carlo simulation will be able to tell how large a proportion of the completely flat serves will be successful, versus a topspin serve, if a number of trials are performed.

5. CONCLUSION

In summary, more successful topspin serve $n = 572$ combinations of impact and racket face angles were found contrary to successful flat serves $n = 42$. The optimum impact angle regarding spin rate were found at 34° , 35° and 36° for junior, recreational and professional tennis players, respectively. Corresponding optimal racket face angles were found at 14° , 18° and 21° which resulted in high velocity serves landing close to the service line. Almost similar impact angles, considering the physiological differences between the players, will make it simple for players and coaches to implement high spin rates for topspin serves. Additionally, impact angles larger than optimum resulted in an accelerated velocity decrease due to the energy loss from sliding friction. Although spin rates from the present collision model are overestimated compared to existing literature, the parabola-like pattern of the spin rate, as a function of the impact angle, is believed to be realistic.

ACKNOWLEDGEMENTS

The authors would like to give a great gratitude to the study's supervisor John Rasmussen for being available and providing crucial guidance when needed.

REFERENCES

- [1] H. Brody, *Tennis Science for Tennis Players*. University of Pennsylvania Press, 1987. DOI: doi: 10.9783/9780812201468.
- [2] J. Carboch, J. Tufano, and V. Süß, "Ball toss kinematics of different service types in professional tennis players," *International Journal of Performance Analysis in Sport*, vol. 18, pp. 1–11, Oct. 2018. DOI: 10.1080/24748668.2018.1519750.
- [3] J. Chow, L. Carlton, Y.-T. Lim, W.-S. Chae, J.-H. Shim, A. Kuenster, and K. Kokobun, "Comparing the pre- and post-impact ball and racquet kinematics of elite tennis players' first and second serves: A preliminary study," eng, *Journal of sports sciences*, vol. 21, no. 7, pp. 529–537, 2003, ISSN: 0264-0414.
- [4] R. Cross, "Effects of friction between the ball and strings in tennis," eng, *Sports engineering*, vol. 3, no. 2, pp. 85–97, 2000, ISSN: 1369-7072.
- [5] R. Cross, "The kick serve in tennis," *Sports Technology*, vol. 4, pp. 1–10, Jan. 2012. DOI: 10.1080/19346182.2012.663534.
- [6] J. Fernandez-Fernandez, T. Ellenbecker, D. Sanz-Rivas, A. Ulbricht, and A. Ferrautia, "Effects of a 6-week junior tennis conditioning program on service velocity," eng, *Journal of sports science medicine*, vol. 12, no. 2, pp. 232–239, 2013, ISSN: 1303-2968.
- [7] G. Fleisig, R. Nicholls, B. Elliott, and R. Escamilla, "Tennis: Kinematics used by world class tennis players to produce high-velocity serves," eng, *Sports biomechanics*, vol. 2, no. 1, pp. 51–64, 2003, ISSN: 1476-3141.
- [8] H. Ghaednia, O. Cermik, and D. B. Marghitu, "Experimental and theoretical study of the oblique impact of a tennis ball with a racket," eng, *Proceedings of the Institution of Mechanical Engineers. Part P, Journal of sports engineering and technology*, vol. 229, no. 3, pp. 149–158, 2015, ISSN: 1754-3371.
- [9] J. A. Glynn, M. A. King, and S. R. Mitchell, "A computer simulation model of tennis racket/ball impacts," eng, *Sports engineering*, vol. 13, no. 2, pp. 65–72, 2011, ISSN: 1369-7072.
- [10] S. Goodwill, J. Douglas, S. Miller, and S. Haake, "Measuring ball spin off a tennis racket," eng, in *The Engineering of Sport 6*, New York, NY: Springer New York, pp. 379–384, ISBN: 0387317732.
- [11] S. R. Goodwill and S. J. Haake, "Spring damper model of an impact between a tennis ball and racket," eng, *Proceedings of the Institution of Mechanical Engineers. Part C, Journal of mechanical engineering science*, vol. 215, no. 11, pp. 1331–1341, 2001, ISSN: 0954-4062.
- [12] S. R. Goodwill, R. Kirk, and S. J. Haake, "Experimental and finite element analysis of a tennis ball impact on a rigid surface," eng, *Sports engineering*, vol. 8, no. 3, pp. 145–158, 2005, ISSN: 1369-7072.
- [13] S. Haake, T. Allen, A. Jones, J. Spurr, and S. Goodwill, "Effect of inter-string friction on tennis ball rebound," eng, *Proceedings of the Institution of Mechanical Engineers. Part J, Journal of engineering tribology*, vol. 226, no. 7, pp. 626–635, 2012, ISSN: 1350-6501.
- [14] S. Haake, M. Carré, and S. Goodwill, "The dynamic impact characteristics of tennis balls with tennis rackets," eng, *Journal of sports sciences*, vol. 21, no. 10, pp. 839–850, 2003, ISSN: 0264-0414.
- [15] S. Haake, S. Goodwill, and M. Carré, "A new measure of roughness for defining the aerodynamic performance of sports balls," *Proceedings of The Institution of Mechanical Engineers Part C-journal of Mechanical Engineering Science*, vol. 221, pp. 789–806, Jul. 2007. DOI: 10.1243/0954406JMES414.
- [16] Y. Kawazoe and Y. Kanda, "Analysis of impact phenomena in a tennis ball-racket system : Effects of frame vibrations and optimum racket design," eng, *JSME international journal. Series C, Dynamics, control, robotics, design and manufacturing*, vol. 40, no. 1, pp. 9–16, 1997, ISSN: 1340-8062.

- [17] D. C. Leigh and W.-Y. Lu, “Dynamics of the interactions between ball, strings, and racket in tennis,” *International Journal of Sport Biomechanics*, vol. 8, no. 3, pp. 181–206, 1992. DOI: 10.1123/ijsb.8.3.181.
- [18] R. Mehta, F. Alam, and A. Subic, “Review of tennis ball aerodynamics,” eng, *Sports technology*, vol. 1, no. 1, pp. 7–16, 2008, ISSN: 1934-6182.
- [19] R. D. Mehta and J. M. Pallis, “The aerodynamics of a tennis ball,” eng, *Sports engineering*, vol. 4, no. 4, pp. 177–189, 2001, ISSN: 1369-7072.
- [20] S. Sakurai, M. Reid, and B. Elliott, “Ball spin in the tennis serve: Spin rate and axis of rotation,” eng, *Sports biomechanics*, vol. 12, no. 1, pp. 23–29, 2013, ISSN: 1476-3141.
- [21] H. Schlarb, B. Kneib, and U. Glitsch, “Modeling of elastic racket properties in the dynamic computer simulation of tennis,” 1998.
- [22] S. N. Sørensen and J. Rasmussen, “Free kick goals in football: An unlikely success between failure and embarrassment,” eng, *Sports engineering*, vol. 21, no. 2, pp. 103–114, 2018, ISSN: 1369-7072.
- [23] A. Štěpánek, “The aerodynamics of tennis balls—the topspin lob,” *American Journal of Physics*, 1987. DOI: doi:10.1119/1.15692.
- [24] M. Yeadon and J. Challis, “The future of performance-related sports biomechanics research,” eng, *Journal of sports sciences*, vol. 12, no. 1, pp. 3–32, 1994, ISSN: 0264-0414.

Worksheet

2-dimensional tennis serves show similar successful mechanical parameter across physiological differences



Kristian H. Grosen, Mads Kousted & Sean L. Treichel

Aalborg Universitet
Speciale Idrætsteknologi

Preface

The purpose of the worksheet is to elaborate on the theoretical and mythological considerations of the article/paper/study above. First, an introduction to various mechanical factors that influences a tennis serve will be presented, then derivatives of the differential equilibrium equations forming the perpendicular and tangential differential systems followed by diagrams of important outcomes from the Python collision model. The reminder of the worksheet will include in-depth recaps of individual mechanical factors mentioned in the beginning.

Aalborg Universitet, June 1, 2021

Indholdsfortegnelse

Preface	3
Chapter 1 Mechanical Factors	5
1.1 Pre-impact	6
1.2 Collision	6
1.3 Post-impact	7
Chapter 2 Python Script	9
2.1 Derivatives of coupled differential equations	9
2.2 Collision model	13
2.3 Flight model	15
Chapter 3 Theory	17
3.1 Collision	17
3.2 Friction	19
3.3 Drag Force	21
3.4 Magnus Force	22
3.5 Computer Simulation	24
Bibliography	27

Mechanical Factors

1

The following section will see a tennis serve being split into three phases to give a general understanding of the mechanical factors. For instance, using geometry while neglecting aerodynamics and gravity, the minimum point of impact for a completely flat serve is found at 2.74 m [1]. This is because several limitations are applied to the game of tennis in order to increase the difficulty of the serve. In the middle of the court, a ball (with radius r) has to pass a net ($.91\text{ m}$ at the center and 1.07 m at the tramlines) and then land inside the diagonal service box with the server standing at a minimum of 11.885 m from the net for the serve to be successful (1.1).

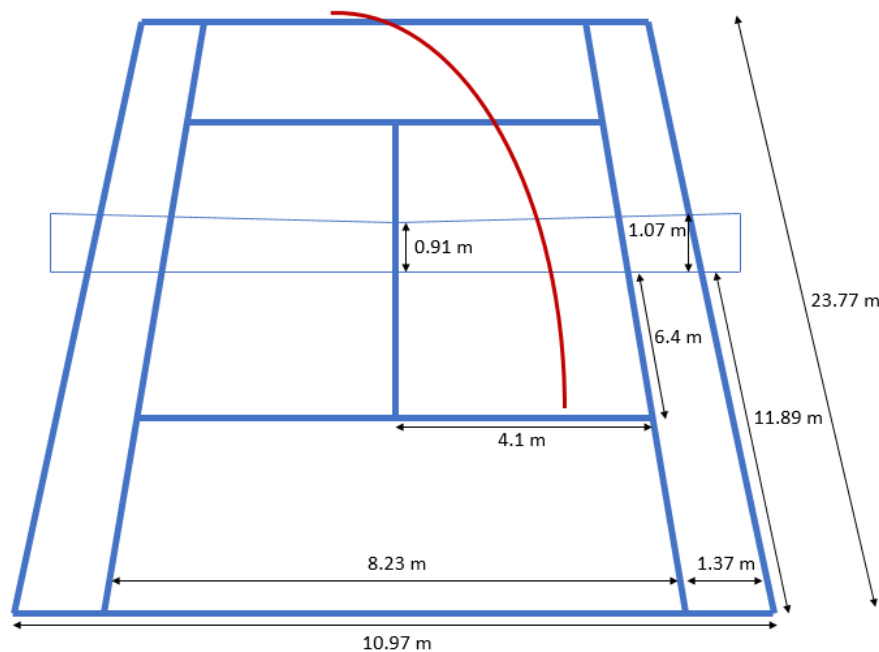


Figure 1.1. Tennis court with corresponding dimensions. The brown line shows a potential ball trajectory for a successful serve.

While a successful flat serve from the minimum point of impact is mathematically easy to accomplish, this is not the case in the real world. Impact height, impact velocity, impact angle (α) and racket face angle (β) are factors that only can vary a few percent to accomplish a completely flat serve [1]. Other Mechanical factors such as aerodynamics, gravitational acceleration and Magnus force also makes a completely flat serve impossible in the real world. Though, in the case of achieving a successful serve, as described above, aerodynamics and gravitational acceleration will benefit the player while Magnus force will

benefit the player if utilized right.

1.1 Pre-impact

For the pre-impact-phase the velocity of the racquet, vertical ball velocity, and ball position just before collision are important mechanical factors. The perpendicular velocity of the racquet is the dominant factor to determine the initial velocity of the ball after impact. The vertical ball velocity will ultimately decide the timing difficulty of the impact, but higher velocity will also induce more ball spin post-impact [2]. The magnitude can be derived from knowing the horizontal velocity of the racquet (a) and the vertical velocity of the ball (b). Suppose the ball is at rest, and the racquet is moving horizontally with velocity a and vertically with velocity b the angle can be derived by:

$$A = \tan^{-1}\left(\frac{a}{b}\right) \quad (1.1)$$

Then the spin rate can found by [2]:

$$S = 1.45aA \quad (1.2)$$

Pre-impact, the ball is subject to wind resistance, also known as drag force, albeit the magnitude is small because of low velocities.

1.2 Collision

For the collision-phase two prominent forces occur - the tangential force (F_f) and the perpendicular force (F_N) [3]. The magnitude of these forces are determined by the racket velocity, β and α (figures 1.2 and 1.3). F_N will generate the translational acceleration while F_f will generate a combination of linear and angular acceleration [3]. Assuming Coulumb friction, the following rule applies for F_f :

$$F_f \leq F_N \mu \quad (1.3)$$

Where μ is the coefficient of friction between the racquet and tennis ball. If α between the racket and ball is zero there will only be generated translational acceleration (1.2).

The margin of error for this example is small, because a small deviation of β will conclude in the ball either hitting the net or being too long at a high racket velocity [1]. To ensure a bigger margin of error, players look to increase α to distribute the total force for both F_N and F_f (1.3).

Generating angular acceleration to the ball will initiate Magnus force after collision with a decrease in translational acceleration [3].

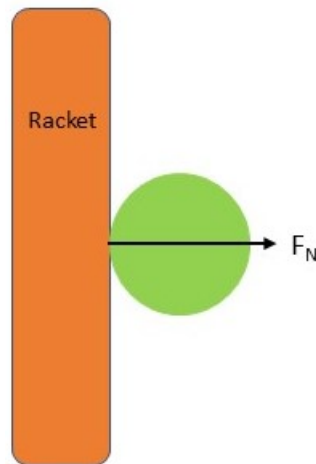


Figure 1.2. Both α and β is zero in this example.

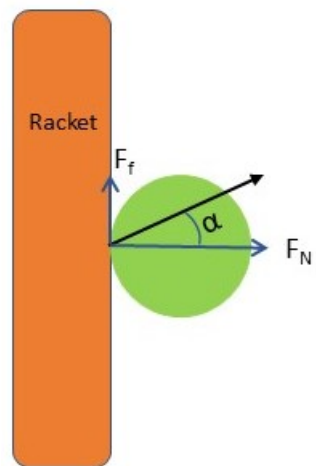


Figure 1.3. Both F_N and F_f will be present if α differs from 0-degrees. In this example, F_f will induce topspin. β is zero.

1.3 Post-impact

Post-impact the ball is subject to much greater drag force, because of the larger velocities compared to pre-impact [4]. Together with the gravitational acceleration, these two forces aid the ball in reaching its preferable destination - inside the tram lines of the tennis court (figure 1.1). Reynolds number Re , which gives an indication of the air flow around the ball during flight, can alter the drag force depending on the magnitude. Metha and Pallis [5] found that for $Re < 150.000$ ($33.8 \frac{m}{s}$) the drag coefficient varies between 0.61 - 0.75 for a Wilson US Open 3 tennis ball. For $Re > 150.000$ they found that the drag coefficient varies slightly, hence an averaged single value was accepted [5]. Magnus force is another factor that will have an effect on the flight trajectory of the ball. Topspin, backspin and sidespin will all alter the trajectory of the flight of the ball with the magnitude of the angular velocity also being a factor together with the translational velocity.

Python Script 2

The process of developing a script to simulate a tennis serve, was first split into two models. The first model was to develop a collision script, that could handle the pre-impact (1.1.1) and collision (1.1.2) phase. While the second model should handle the post-impact (1.1.3) phase. The perpendicular and tangential forces, accelerations, (angular) velocities and positions were all obtained from the coupled differential equations in section 2.2 of the article and derived in section 2.1 of the worksheet. For all figures (2.2-2.7) shown in sections 2.2 and 2.3: racket velocity = 40m/s , $\alpha = 21^\circ$ and $\beta = 35^\circ$.

2.1 Derivatives of coupled differential equations

In section 2.2 of the article, 11 differential equations (equations 7-11 and 13-18) were derived based on Newtonian laws to form two separate differential systems for perpendicular (x) and tangential forces (y) (equations 12 and 19). In this section an assessment of the calculations leading to the differential systems is performed. Solving for \dot{x} and \dot{y} , the target is to have every x (perpendicular) and y (tangential) occupying its own link.

2.1.1 x-matrix

Initially, a second order differential system in the article was made for x -values with three equations containing three unknown variables (equations 7-9). These three equations were used on the basis of figure 2.1.

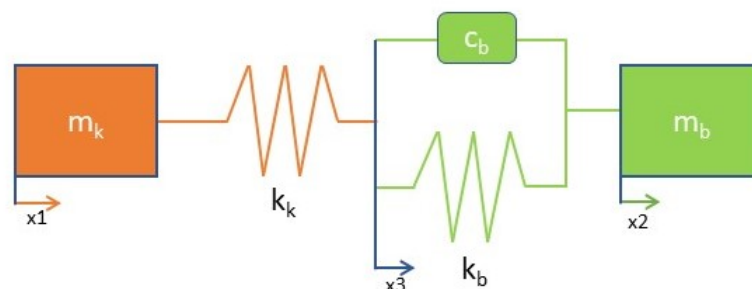


Figure 2.1. Shows the racket mass as m_K acting on the ball m_B through the racket's spring stiffness as K_K . While the ball's spring stiffness is K_B and damper is C_b .

In order to increase the accuracy of the calculations, the differential system was reduced to a first order system. A substitution was made which led to the creation of two new variables, x_4 and x_5 . From equations 10 and 11, \dot{x}_1 and \dot{x}_2 were derived:

$$\dot{x}_1 = x_4 \quad (2.1)$$

$$\dot{x}_2 = x_5 \quad (2.2)$$

From equations 7 and 10, \dot{x}_4 was derived:

$$\begin{aligned} m_k \dot{x}_4 &= -(x_1 - x_3)k_k \\ \implies \dot{x}_4 &= \frac{-x_1 k_k + x_3 k_k}{m_k} \\ \implies \dot{x}_4 &= \frac{-x_1 k_k}{m_k} + \frac{x_3 k_k}{m_k} \\ \implies \dot{x}_4 &= -\frac{k_k}{m_k} x_1 + \frac{k_k}{m_k} x_3 \end{aligned} \quad (2.3)$$

Taken from the top, m_k is divided on both sides and k_k is multiplied into the parenthesis. Next, the fraction is split into two separate fractions, because of the common denominator. Lastly, x_1 and x_3 is put next to the fraction for clarity regarding the forthcoming matrix notation in the article.

From equations 9-11, \dot{x}_5 was derived:

$$\begin{aligned} m_k \dot{x}_4 &= -m_b \dot{x}_5 \\ \implies m_k \left(-\frac{k_k}{m_k} x_1 + \frac{k_k}{m_k} x_3 \right) &= -m_b \dot{x}_5 \\ \implies -k_k x_1 + k_k x_3 &= -m_b \dot{x}_5 \\ \implies \frac{-k_k x_1 + k_k x_3}{-m_b} &= \dot{x}_5 \\ \implies -\frac{k_k x_1}{-m_b} + \frac{k_k x_3}{-m_b} &= \dot{x}_5 \\ \implies \frac{k_k}{m_b} x_1 - \frac{k_k}{m_b} x_3 &= \dot{x}_5 \end{aligned} \quad (2.4)$$

Here, \dot{x}_4 is replaced with the notation from equation 2.3. With m_k being multiplied into the parenthesis will entail m_k is removed from the equation. After m_b is divided on both sides, the derivation of \dot{x}_5 follows the same path as for \dot{x}_4 .

Lastly, from equations 8 and 11, \dot{x}_3 was derived:

$$\begin{aligned}
m_b \dot{x}_5 &= (x_3 - x_2)k_b + (\dot{x}_3 - \dot{x}_5)c_b \\
\implies m_b \left(\frac{k_k}{m_b} x_1 - \frac{k_k}{m_b} x_3 \right) &= (x_3 - x_2)k_b + (\dot{x}_3 - \dot{x}_5)c_b \\
\implies k_k x_1 - k_k x_3 &= k_b x_3 - k_b x_2 + (\dot{x}_3 - \dot{x}_5)c_b \\
\implies k_k x_1 - k_k x_3 - k_b x_3 + k_b x_2 &= (\dot{x}_3 - \dot{x}_5)c_b \\
\implies \frac{k_k x_1 + k_b x_2 - (k_k x_3 + k_b x_3)}{c_b} &= \dot{x}_3 - \dot{x}_5 \\
\implies \frac{k_k}{c_b} x_1 + \frac{k_b}{c_b} x_2 - \frac{(k_k + k_b)}{c_b} x_3 + \dot{x}_5 &= \dot{x}_3
\end{aligned} \tag{2.5}$$

First, \dot{x}_5 is replaced with the notation from equation 2.4 and like in equation 2.3 this will entail that m_b is removed. At the same time, k_b is multiplied into the parenthesis and afterwards moved to the left side of the equal sign by addition and subtraction. Next, c_b is divided on both sides and the two x_3 links are moved together inside a joint parenthesis. Lastly, the fraction is split into three separate fractions, because of the common denominator and \dot{x}_5 is added to both sides to isolate \dot{x}_3 .

2.1.2 y-matrix

A similar second order differential system was made for the y -values and applied the same accuracy optimization. The tangential differential system had an additional row (six in total) because of the need to specify angular acceleration. This entails the incorporation of the balls mass moment of inertia (I) - confer Newton's second law for rotating objects

$$I = \frac{2}{3}mr^2 \tag{2.6}$$

and the balls radius (r).

Reducing the second order differential system to a first order system led to a substitution, hence the derivation of three new variables, y_4 , y_5 and y_6 . From equations 16-18, \dot{y}_1 , \dot{y}_2

and y_3 were derived:

$$\dot{y}_1 = y_4 \quad (2.7)$$

$$\dot{y}_2 = y_5 \quad (2.8)$$

$$\dot{y}_3 = y_6 \quad (2.9)$$

From equations 13 and 16, \dot{y}_4 was derived:

$$\begin{aligned} m_k \dot{y}_4 &= -(y_1 - y_2 - ry_3)k - (y_4 - y_5 - ry_6)c \\ \implies m_k \dot{y}_4 &= -ky_1 + ky_2 + kry_3 - cy_4 + cy_5 + cry_6 \\ \implies \dot{y}_4 &= \frac{-ky_1 + ky_2 + kry_3 - cy_4 + cy_5 + cry_6}{m_k} \\ \implies \dot{y}_4 &= -\frac{k}{m_k}y_1 + \frac{k}{m_k}y_2 + \frac{kr}{m_k}y_3 - \frac{c}{m_k}y_4 + \frac{c}{m_k}y_5 + \frac{rc}{m_k}y_6 \end{aligned} \quad (2.10)$$

First, k and c are multiplied into the parenthesis with m_k then being divided on both sides. Next, the fraction is split into six separate fractions, because of the common denominator, with y_n subsequently put next to the fraction for clarity regarding the forthcoming matrix notation in the article.

From equations 14, 16 and 17, \dot{y}_5 is derived:

$$\begin{aligned} m_b \dot{y}_5 &= -m_k \dot{y}_4 \\ \implies m_b \dot{y}_5 &= -m_k \left(-\frac{k}{m_k}y_1 + \frac{k}{m_k}y_2 + \frac{kr}{m_k}y_3 - \frac{c}{m_k}y_4 + \frac{c}{m_k}y_5 + \frac{rc}{m_k}y_6 \right) \\ \implies m_b \dot{y}_5 &= ky_1 - ky_2 - kry_3 + cy_4 - cy_5 - rcy_6 \\ \implies \dot{y}_5 &= \frac{ky_1 - ky_2 - kry_3 + cy_4 - cy_5 - rcy_6}{m_b} \\ \implies \dot{y}_5 &= \frac{k}{m_b}y_1 - \frac{k}{m_b}y_2 - \frac{kr}{m_b}y_3 + \frac{c}{m_b}y_4 - \frac{c}{m_b}y_5 - \frac{rc}{m_b}y_6 \end{aligned} \quad (2.11)$$

First, y_4 is replaced with the notation from equation 2.10 which will then entail that m_k is removed. The remaining steps follows the same procedure as in equation 2.10.

From equations 15, 17 and 18, y_6 is derived:

$$\begin{aligned}
 I\dot{y}_6 &= rm_b\dot{y}_5 \\
 \implies I\dot{y}_6 &= rm_b\left(\frac{k}{m_b}y_1 - \frac{k}{m_b}y_2 - \frac{kr}{m_b}y_3 + \frac{c}{m_b}y_4 - \frac{c}{m_b}y_5 - \frac{rc}{m_b}y_6\right) \\
 \implies I\dot{y}_6 &= rky_1 - rky_2 - r^2ky_3 + rcy_4 - rcy_5 - r^2cy_6 \tag{2.12} \\
 \implies \dot{y}_6 &= \frac{rky_1 - rky_2 - r^2ky_3 + rcy_4 - rcy_5 - r^2cy_6}{I} \\
 \implies \dot{y}_6 &= \frac{rk}{I}y_1 - \frac{rk}{I}y_2 - \frac{r^2k}{I}y_3 + \frac{rc}{I}y_4 - \frac{rc}{I}y_5 - \frac{r^2c}{I}y_6
 \end{aligned}$$

First, y_5 is replaced with the notation from equation 2.11 which will entail the removal of m_b . The remaining steps follows the same procedure as in equation 2.11.

2.2 Collision model

In the previous section the derivation of the coupled differential equations were elaborated, while in this section the computational outputs regarding forces, accelerations, velocities and positions are presented for the collision model.

The positions in the perpendicular axis indicated when the ball and racket were colliding. The racket had a initial value of -0.02 m behind the ball at 0.0 m . The collision was indicated by the rackets position being greater than the position of the ball, as seen in figure 2.2 (left).

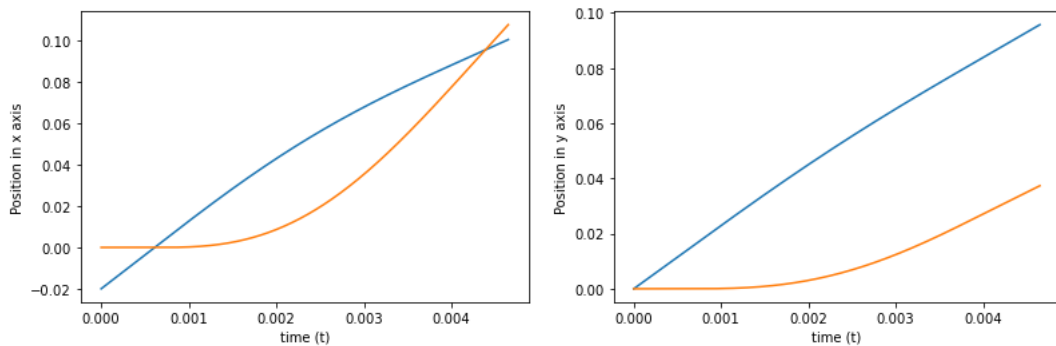


Figure 2.2. Positions of racket (Blue) and ball (Orange).

For the racket and ball to collide an initial velocity of the racket was necessary. The velocities in both axis for racket and ball is seen in figure 2.3. To derive the perpendicular (equation 2.13) and tangential (equation 2.14) racket velocity simple trigonometry was used:

$$v_x = 40 * \cos(35) \tag{2.13}$$

$$v_y = 40 * \sin(35) \tag{2.14}$$

While the initial racket and ball velocity are constant the accelerations will be equal to zero, until collision, as presented in figure 2.4. The ball will in the first time step of collision be accelerated by the velocity of the racket, where forces are equally distributed between the racket and the ball (figure 2.5) - confer Newton's third law. This is then used to predict the velocity (figure 2.3) and subsequently the position (figure 2.2) of the racket and ball.

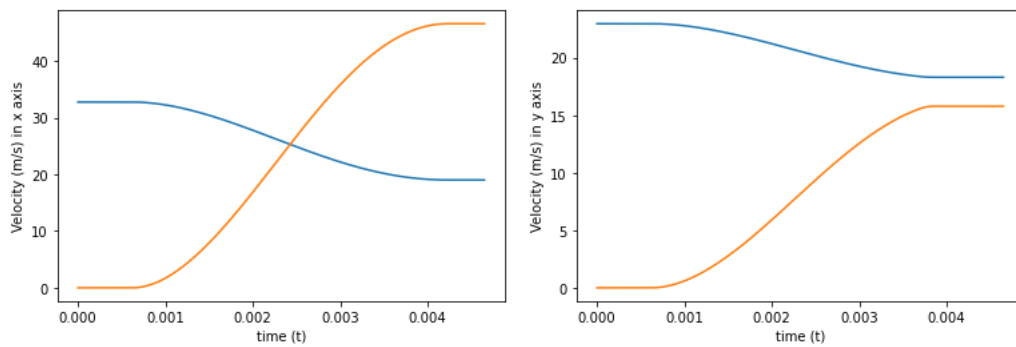


Figure 2.3. Velocities of racket (Blue) and ball (Orange).

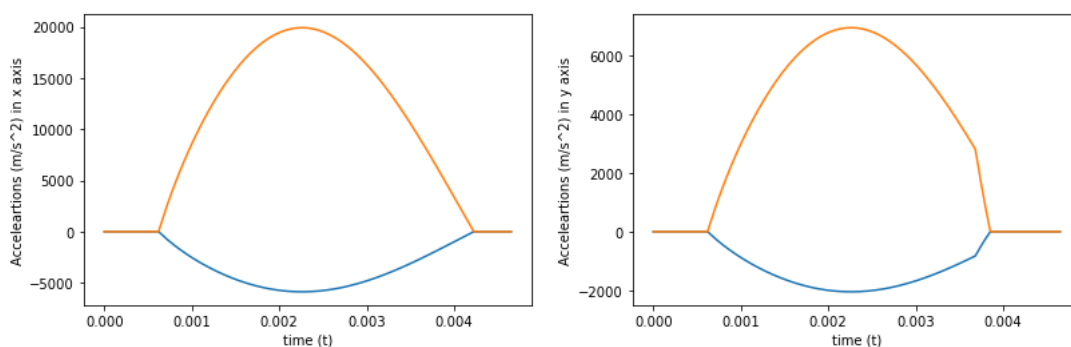


Figure 2.4. Accelerations of racket (Blue) and ball (Orange).

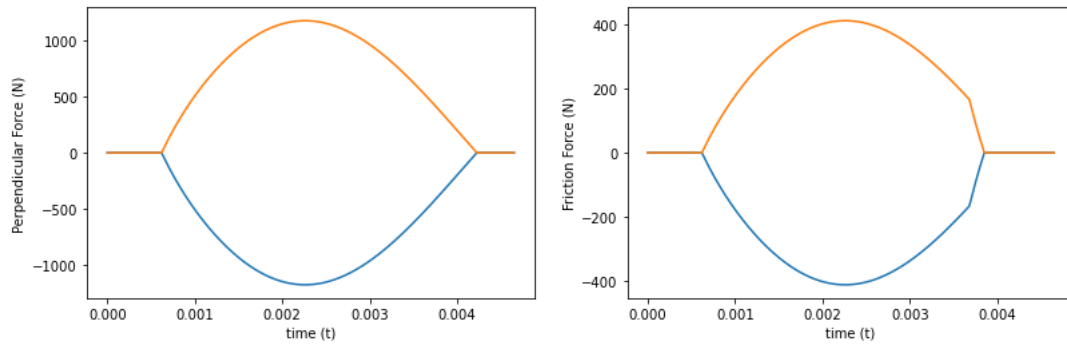


Figure 2.5. Left: Perpendicular forces of racket (Blue) and ball (Orange). Right: Tangential forces of racket (Blue) and ball (Orange).

2.3 Flight model

After the collision model has run, ω (figure 2.6(Right)) and the rotated velocity components (figure 2.6(Left)) of the ball are implemented in the flight model to determine the trajectory of the ball. The rotated velocities are given from equation 22 on the basis of β . The unit of ω is rad/s and is transformed to revolutions per minute (RPM) by: $\frac{\omega 60}{2\pi}$. The increase in RPM happens due to the tangential accelerations and forces.

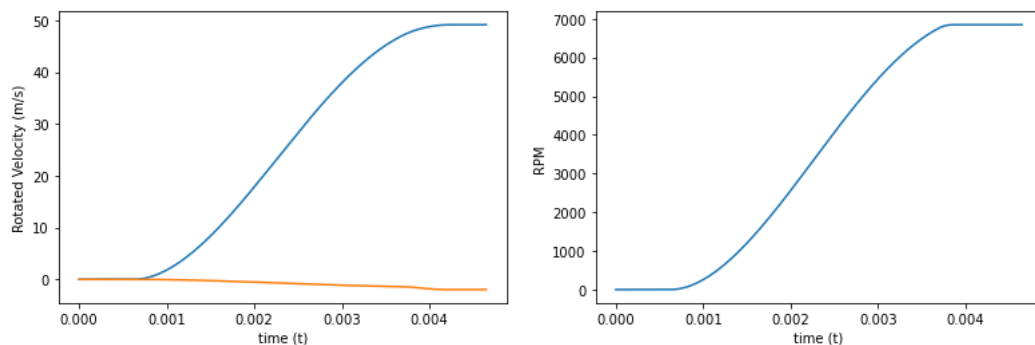


Figure 2.6. Left: Rotated velocity for x component (Blue) and y component (Orange). Right: The amount of spin through collision in RPM

The amount of spin and velocity, will alter the drag and lift coefficient, which determine the amount of drag and Magnus force present in the flight model, as presented in figure 2.6. The drag force decreases over flight time, as seen in figure 2.7. This is mainly caused by the decrease of velocity through the flight time. The Magnus force is defined as topspin when negative, indicated by figure 2.7 the Magnus force decreases over flight time, which is mainly a result of a decrease in the velocity.

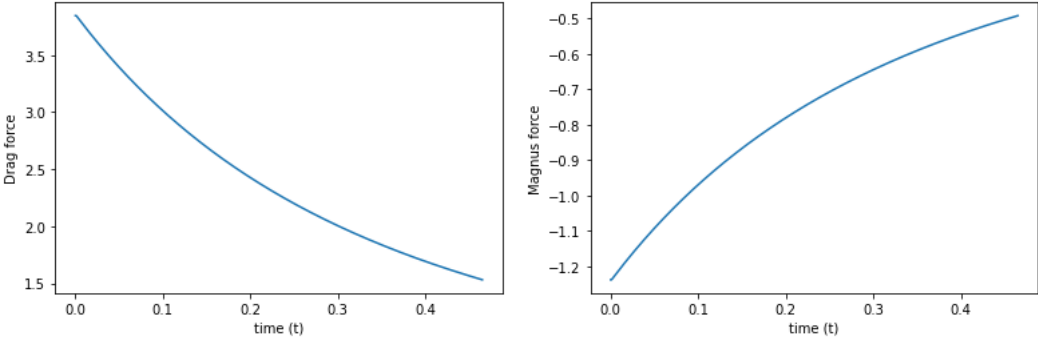


Figure 2.7. Left: Drag force. Right: Magnus force

Theory 3

The above mentioned simulation models are in each and every step based on theoretical approximations of different mechanical factors. Background knowledge will be presented and elaborated regarding the collision between racket and ball and the flight of the ball.

3.1 Collision

Newtonian laws were used to derive the coupled differential equations outlined in section 2.2 of the article and section 2.1 of the worksheet. In the following section, general knowledge for the collision between two objects using Newtonian laws is outlined.

In mechanics, impulse denotes the collision between two bodies and is based on Newton's second law:

$$F = ma \tag{3.1}$$

Where F is force, m is mass and a is acceleration. Impulse is assigned the symbol p and is defined as the product of mass and velocity (v):

$$p = mv \tag{3.2}$$

The relationship between impulse and Newton's second law is shown as:

$$F = ma = m \frac{\Delta v}{\Delta t} = \frac{\Delta(mv)}{\Delta t} = \frac{\Delta p}{\Delta t} = p \tag{3.3}$$

This means that F is the time derivative of p , and p can be perceived as the effect of the resulting force summed (integrated) over a period of time [6]:

$$p = \frac{F}{\Delta t} \tag{3.4}$$

The impulse is preserved in a system if there are no external forces acting, compare the laws of Newton, though complicated internal forces can be present. The impulse of a system can not be changed if the acceleration is zero and from that we get, the principle of linear momentum [6; 7]:

$$\dot{p} = ma = 0 \tag{3.5}$$

Or

$$p_1 = p_2 \quad (3.6)$$

For a system consisting of two objects, A and B, the impulse theorem can be derived as:

$$m_A v_{A1} + m_B v_{B1} = m_A v_{A2} + m_B v_{B2} \quad (3.7)$$

Using the conservation laws of momentum and energy, much information about the motion after collision can be determined in terms of information before collision. Collisions with rigid object, where all the kinetic energy is conserved, is referred to as elastic collision. If none of the kinetic energy is conserved in a collision, it is referred to as an inelastic collision [7]. Collisions are rarely completely elastic. Usually some of the kinetic energy is lost to friction or plastic deformation. The energy loss is described by the coefficient of restitution [6].

3.1.1 Coefficient of restitution

In practice, collisions are rarely completely elastic or inelastic, since part of the kinetic energy is converted into other forms of energy. The loss in kinetic energy is described by the coefficient of restitution. The coefficient of restitution can be found using physics' definition of work and by dividing the collision into two phases. The first part is the deformation phase, which take place from the moment the two objects come into contact with each other and until the deformation is at the maximum. The second phase is the restitution phase and is from where the deformation has reached its maximum, and until the two objects release each other again.

In physics, work is defined by force along displacement. If the objects return to their original shapes, the displacement is the same for both the deformation phase and the restitution phase. How much of the energy is conserved thus depends on the forces summed over the restitution time, corresponding to the forces summed over the deformation time. If we define the time interval for the deformation from 0 to t_0 , and the restitution happens from t_0 to t . Thus, the effects of the deformation force (F_d) and the restitution force (F_r) on each object, can be described as following:

$$\int_0^{t_0} F_d dt \quad (3.8)$$

$$\int_{t_0}^t F_r dt \quad (3.9)$$

The integral of force over time is the same as the change in impulse. From this we get following equations for object A, which is the same for object B, since the two objects stick

together at this time:

$$\int_0^{t_0} F_d dt = [m_A v_A(t)]_0^{t_0} = m_A(v_0 - v_{A1}) \quad (3.10)$$

$$\int_{t_0}^t F_r dt = [m_A v_A(t)]_{t_0}^t = m_A(v_{A2} - v_0) \quad (3.11)$$

The coefficient of restitution of object A, can be calculated from this as the ratio between the effect of the restitution forces and the effect of the deformation forces:

$$e_A = \frac{\int_{t_0}^t F_r dt}{\int_0^{t_0} F_d dt} = \frac{m_A(v_{A2} - v_0)}{m_A(v_0 - v_{A1})} = \frac{v_{A2} - v_0}{v_0 - v_{A1}} \quad (3.12)$$

The same can be done for object B:

$$e_B = \frac{\int_{t_0}^t F_r dt}{\int_0^{t_0} F_d dt} = \frac{v_{B2} - v_0}{v_0 - v_{B1}} \quad (3.13)$$

The coefficient between the two integrals is the same for both objects and thus the coefficients of restitution for the objects are equal:

$$e_A = e_B \Rightarrow \frac{v_{A2} - v_0}{v_0 - v_{A1}} = \frac{v_{B2} - v_0}{v_0 - v_{B1}} \quad (3.14)$$

Of which a common coefficient of restitution can be set, by eliminating v_0 :

$$e = \frac{v_{B2} - v_{A2}}{v_{A1} - v_{B1}} \quad (3.15)$$

That means, the coefficient of restitution can be calculated simply by knowing the velocities of the objects before and after the collision. If e is equal to 1 it is a fully elastic collision. Conversely if e is equal to 0, it is a completely inelastic collision.

3.2 Friction

The previous section 3.1 described the perpendicular collision between two objects. In tennis, the collision is always a combination of perpendicular and tangential forces, which will entail friction forces between the string bed of the racket and the ball.

Leonardo Da Vinci (1452-1519) was the first to quantify friction. He stated two basic laws of friction: The force of friction is directly proportional to the applied load. The force of friction is independent of the apparent area of contact for a given load. A few hundred years later, Leonard Euler (1707-1783) provided a clear distinction between static and dynamic friction. Two years after Leonard Euler's death, Charles Augustin Coulomb (1736-1806) described for the first time the formula of frictional force:

$$F_f = \mu F_N \quad (3.16)$$

F_f is the tangential friction force, F_N is the perpendicular force, μ is the coefficient of friction and is a constant which depends on the combination of materials in contact with each other. This is also called coloumb-friction. No materials have a completely smooth surface, which is why there will always be small roughnesses and gaps. It is these roughnesses and gaps that create chemical or physically adhesive bonds that must be overcome with a certain force, which depends on the material and load [6; 8].

μ is an important parameter in the game of tennis. Without it, the amount of spin it is possible to impart to the ball will be inconsiderable [9]. Now, for a tennis serve, as written in chapter 1, ball spin is not necessary to accomplish a successful serve, but it will make it possible to achieve high serve velocities along with a larger margin of error. Generally, a higher μ will entail more spin after collision, but this is also dependent on α and racket velocity [9]. Furthermore, it will also entail a greater rebound angle as seen when the ball bounces of the grass at Wimbledon compared to the Parisian clay at Roland Garros [9] - with the latter having the largest μ .

3.2.1 Friction types in tennis

Generally all friction types depends on F_N , that pushes the objects together, and μ (equation 3.16). When an impact occurs, F_N is compressing the ball into the strings, which will stretch the strings and thereby increase friction [9]. The strings will come to a halt and start to return to its original position, at this moment static friction has to be overcome [9], for the dynamic friction to occur.

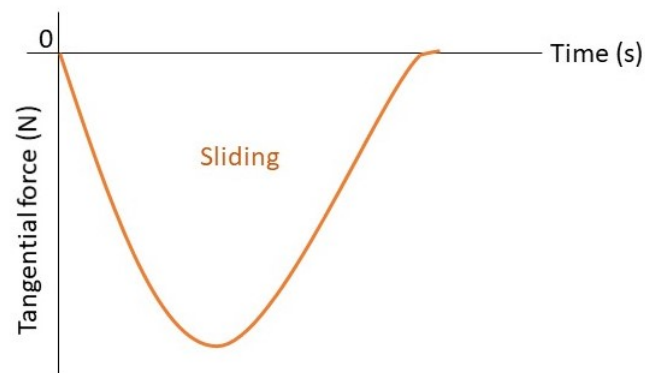


Figure 3.1. A scenario where the ball slides throughout the impact.

When the transition from static to dynamic occur, the ball will either experience a sliding or rolling friction. Sliding friction will always occur for an oblique impact and will remain throughout the impact the frictional force is too low [10]. For sliding friction, the tangential force is negative for the majority and it will rebound with increased spin and decreased velocity. For an impact consisting entirely of sliding friction, the tangential force will stay negative and reaches zero at the end of the impact (figure 3.1).

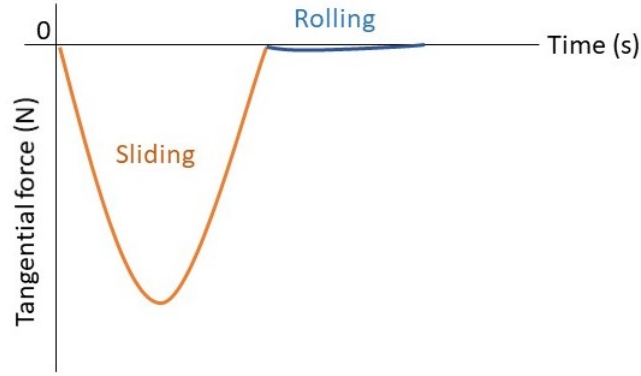


Figure 3.2. A scenario where the ball transits from sliding friction (orange) to rolling friction (blue).

If the tangential force reaches zero before the end of impact, F_f is large enough to transit the ball from sliding friction to rolling friction (figure 3.2). With a sufficient F_f during rolling friction spin will increase [10].

3.3 Drag Force

Having covered the collision between a tennis racket and ball, the attention is moved towards the forces that act on a tennis ball in flight. First the drag force is covered followed by the Magnus force.

In the aspect of a ball's trajectory the drag force plays an important role. The Drag force can simply be explained as following; when an object moves through a medium, it collides with molecules, which decreases the speed[11]. This can be shown with following equation:

$$F_D = \frac{1}{2}C_D A \rho v^2 \quad (3.17)$$

Where v is the ball velocity, A is the cross-sectional area of the ball, ρ is the density of the medium and C_D is the drag coefficient. The average drag coefficient for new tennis balls varies between 0.55 and 0.65 in the absence of spin [4]. According to wind tunnel experiments, a decrease of C_D occurs until obtaining a velocity of approximately 33 m/s, which will result in a relative constant C_D [12].

While a new ball will have a felt fabric cover, which gives it a rough surface and a C_D between 0.55 and 0.65 [4], a very used ball (1500 impacts) will have a smoother surface and experience a decrease in drag coefficient of 0.04 depending on the velocity [13]. A third scenario is a "fluffed up" ball, which is where the felt fabric of the ball will start to fluff [14]. This will result in a higher drag coefficient [14], which is one of the reasons why new balls are provided every 9th game in professional tennis.

In tennis, a flat serve is determined as a serve with very little spin transferred to the ball, in all other shots and serves, spin will be involved. The drag coefficient for spinning balls is greater than for non-spinning balls. The increased drag force for a spinning ball has been quantified by Stepanek [15]:

$$C_D = 0.55 + \frac{1}{[22.5 + 4.2(\frac{v}{r\omega})^h]^p} \quad (3.18)$$

Where h and p are constant values of 2.5 and 0.4, respectively. This leads to another parameter in aerodynamics that will influence the trajectory of a tennis ball, namely the Magnus force.

3.4 Magnus Force

Magnus effect describes the influence of air currents on the trajectory of a flying ball. While a ball travels through the air with an initial straight path it will become curved, because of the Magnus force and the gravitational acceleration. For a topspin ball there will be an increased pressure on the top side of the ball and a lower pressure on the bottom side, which pushes the ball downwards (figure 3.3) and vice versa with a backspin ball, which pushes the ball upwards.

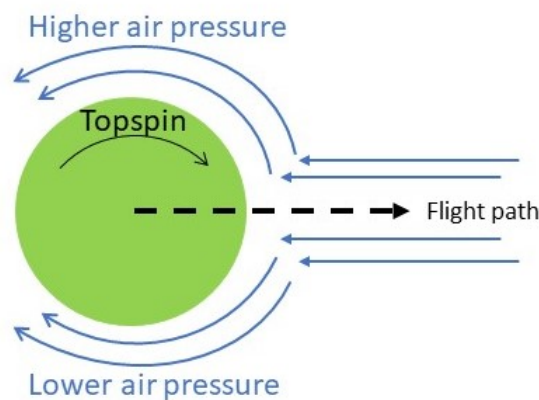


Figure 3.3. Air flow for a ball with topspin.

The different axis of spin can be seen in figure 3.4. Here, a) is topspin or backspin, b) is sidespin and c) is a combination of either topspin or backspin and sidespin. The degree of the axis tilt has been researched by Cross [2], and it is important to understand that pure topspin, backspin or sidespin is practically impossible.

To theoretically examine the Magnus force, the following equation is used:

$$F_M = \frac{1}{2} C_L A \rho v^2 \quad (3.19)$$

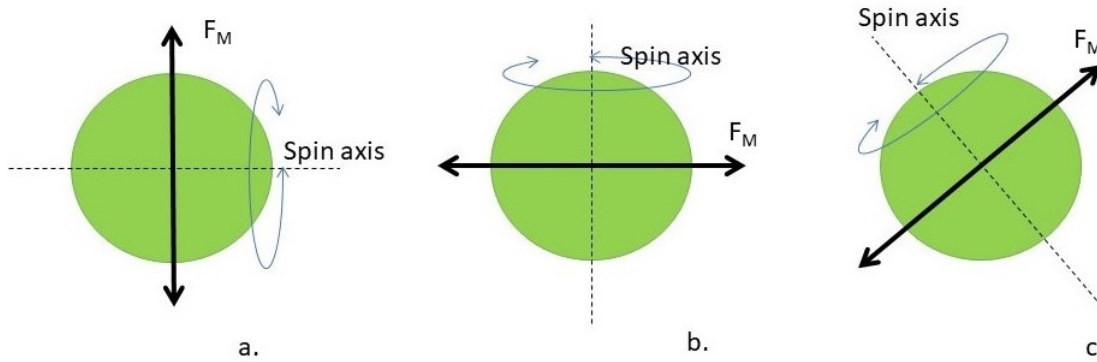


Figure 3.4. The Magnus force acting perpendicular to the spin axis.

Where C_L is the lift coefficient and is given by the following equation:

$$C_L = \frac{1}{2 + \frac{v}{r\omega}} \quad (3.20)$$

From equation 3.20 it can be seen that the lift coefficient increases with the magnitude of ω , which can be influenced by the player by altering α .

In equation 3.19 v is squared in the nominator, which means that the Magnus force depends more on v than ω . Assuming a player can hit with a constant angular velocity, the magnitude of the Magnus force is defined by the magnitude of v , which in turn entails that a greater v results in greater Magnus force.

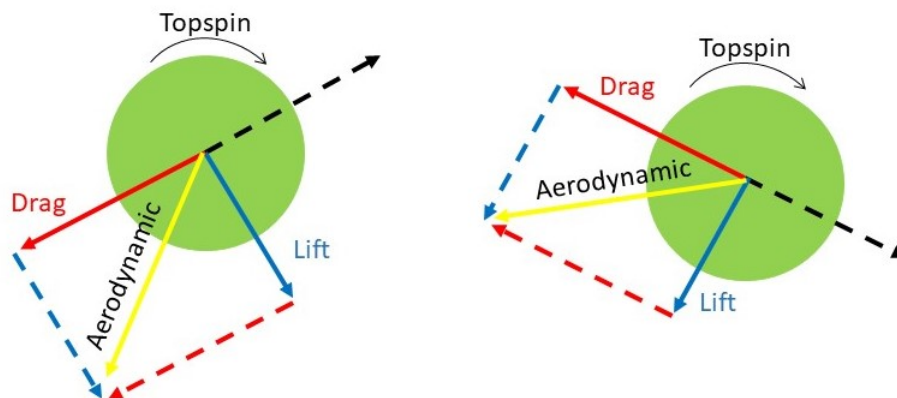


Figure 3.5. The aerodynamic forces acting on a topspin serve. with lift force as blue, drag forces as red and the flight path as black, while the summation of the forces is the yellow arrow.

As seen in figures 3.4 and 3.5 the Magnus force always acts perpendicularly to the drag force and the spin axis. A net force of the drag and Magnus force are shown as the aerodynamic arrow in figure 3.5. A total net force would include the gravitational force

acting on the ball. A serve with topspin will drop faster and hit the court with a steeper angle than a non-spinning ball (flat serve).

3.5 Computer Simulation

In order to analyse the mechanical factors described in the sections above, computer simulation was used. The following section will cover how computer simulations is used to perform forward dynamics.

Computer simulations are commonly used for analyzing bridges, buildings, and machines, but also applicable for biomechanics. With the use of computer simulations, it can be divided into different tools or ways for analyzing the specific scenario such as aerodynamics for analyzing the air flow of an airplane or a tennis ball, rigid dynamics for analyzing forces in a machine or the force in deltoideus when performing a tennis serve, solid mechanics based on finite elements to analyze stiffness properties of pillars in a building or the load on a string bed when serving.

The basis of computer simulations is calculating equations based on the initial information for the specific scenario, which will affect which tool of simulation that will be used. With the initial information of a tennis serve and when trying to simulate a serve based on known forces from the racket to the ball, the tool of simulation is the rigid dynamics, since it can be used to perform a forward dynamic simulation.

3.5.1 Forward dynamics

Forward dynamic simulations are based on knowing the forces acting on the body which can be derived from Newtons second Law. Which also has been stated up in the collision section (3.1). With use of Newtons second law and knowledge of the force and the mass we can determine the acceleration which basically tells us the motion [16].

$$a = \frac{F}{m} \quad (3.21)$$

While these simple sizes can be set in a mathematical model to simulate a simple movement, it can be further developed into a multidimensional model with multiple forces and result in a simulation of a motion or and a collision. The multidimensional sizes of forces can be given as vectors or moments, masses as point mass or a matrix of mass inertia moments and accelerations as angle accelerations or space vector. While the acceleration is known the velocity and position (s) of the body can be derived by a simple integration of time, as seen in the following equations [16]:

$$v(t) = v(0) + \int_0^t a(t)dt \quad (3.22)$$

$$s(t) = s(0) + \int_0^t v(t)dt \quad (3.23)$$

Forward dynamic and other simulation tools can be set up in a coded mathematical model in a computer-aided engineering software such as Python.

3.5.2 Boundary conditions

When performing computer simulations, the sky is the limit for the number of combinations. These limitless combinations must acquire a set of boundary conditions to set a realistic simulation. For this study the simulation model boundaries are based on different physiological capabilities regarding professional, recreational and junior tennis players. Specifically, the individual constant values were impact heights of 3, 2.8 and 2.2 *m*, respectively and racket velocities of 40, 30 and 25 *m/s*, respectively [17; 18]. As the physiology has some boundaries for the serve, the tennis racket has as well, in form of material properties that varies. The variation of the rackets parameters are primarily based on string parameters, since the frame is not incorporated in the simulation. The main string bed parameters which effect the serve are, the stiffness and μ [19]. These factors are again affected by material type, diameter of the strings, string tension and racquet head size. Adjusting the string tension in a range of what is commonly used (28 *kg* - 22 *kg*) will only see a velocity increase of about 0.7 % for a serve at the lowest tension compared to the highest [9]. In modern tennis, strings are made from polyester, nylon and natural gut. The stiffest of the three material types is polyester. For a modern racket the mass varies between, 240 - 380 *g*, and by increasing the mass, the velocity and topspin of the ball can increase [19].

Bibliography

- [1] Brody H. Tennis Science for Tennis Players. University of Pennsylvania Press; 1987. Available from: <https://doi.org/10.9783/9780812201468>.
- [2] Cross R. The kick serve in tennis. Sports Technology. 2012 01;4:1–10.
- [3] Cross R, Lindsey C. Measurements of drag and lift on tennis balls in flight. Sports engineering. 2014;17(2):89–96.
- [4] Mehta R, Alam F, Subic A. Review of tennis ball aerodynamics. Sports technology. 2008;1(1):7–16.
- [5] Mehta RD, Pallis JM. The aerodynamics of a tennis ball. Sports engineering. 2001;4(4):177–189.
- [6] Sørensen JRMKJJSN. Introduktion til biomekanik for idrætsstuderende. Institut for Mekanik og Produktion; 2013.
- [7] Radi HA, Rasmussen JO. Principles of Physics: For Scientists and Engineers. 2013th ed. Undergraduate Lecture Notes in Physics. Berlin, Heidelberg: Springer Berlin Heidelberg;.
- [8] Kietzig AM, Hatzikiriakos SG, Englezos P. Physics of ice friction. Journal of applied physics. 2010;107(8):081101–081101–15.
- [9] Cross R. Effects of friction between the ball and strings in tennis. Sports engineering. 2000;3(2):85–97.
- [10] Allen T, Haake S, Goodwill S. Effect of friction on tennis ball impacts. Proceedings of the Institution of Mechanical Engineers Part P, Journal of sports engineering and technology. 2010;224(3):229–236.
- [11] Lindsey HBRCC. The Physics and Technology of Tennis;.
- [12] Mehta RD. Sport Aerodynamics. International centre for Mechanical Sciences. Springer Wien New York; 2008.
- [13] Goodwill SR, Haake SJ. Spring damper model of an impact between a tennis ball and racket. Proceedings of the Institution of Mechanical Engineers Part C, Journal of mechanical engineering science. 2001;215(11):1331–1341.

-
- [14] Chadwick SG, Haake S. The drag coefficient of tennis balls. *Proceedings of the 3rd International Conference on the Engineering of Sport*. 2000 01;p. 169–176.
- [15] Štěpánek A. The aerodynamics of tennis balls—The topspin lob. *American Journal of Physics*. 1987;.
- [16] Rasmussen J. *Lærebog i biomekanik*. International centre for Mechanical Sciences. Munksgaard; 2018.
- [17] Carboch J, Tufano J, Süß V. Ball toss kinematics of different service types in professional tennis players. *International Journal of Performance Analysis in Sport*. 2018 10;18:1–11.
- [18] Fernandez-Fernandez J, Ellenbecker T, Sanz-Rivas D, Ulbricht A, Ferrautia A. Effects of a 6-week junior tennis conditioning program on service velocity. *Journal of sports science medicine*. 2013;12(2):232–239.
- [19] Allen TB, Haake SJ, Goodwill SR. Effect of tennis racket parameters on a simulated groundstroke. *Journal of sports sciences*. 2011;29(3):311–325.